UCLouvain

École polytechnique de Louvain

Experimental testing of a sensorimotor origin of saccadic suppression compared with a control task

Author: **Marie Romain**
Supervisor: **Frédéric Crevecoeur**
Readers: **Michael Andres, Florence Blondiaux, Frédéric Crevecoeur, Philippe Lefèvre**
Academic year 2021–2022
Master [120] in Biomedical Engineering

Acknowledgments

First, I would like to thank my supervisor, professor Frédéric Crevecoeur, for giving me the opportunity to work on this subject, this gave me an insight into the world of academic research. His experience and hindsight in his advice helped me at the best times

I would also like to thank Florence Blondiaux, for her help and advice, but also for her constant follow-up and understanding.

A special thanks to Guillaume Etienne and Philippe Quirynen for their meticulous proofreading and their advice regarding the writing process.

In addition, I would like to thank all my friends who gave their time and took part in the experiment.

And finally, I want to deeply thank my parents, friends and family for their unfailing support throughout my whole curriculum and during my master's thesis.

Abstract

Saccadic suppression has been studied for a long time and is a phenomenon during which the brain selectively blocks the visual signal during saccadic eye movements. The general opinion is that its purpose serves the stabilization of our perception, which, would be otherwise disturbed by the movement. Even though this explanation seems convincing, it presents some inconsistencies in terms of timing and intensity.

A recent theoretical model of saccadic control, sharing perception and sensorimotor resources, faithfully reproduces the behaviour of real saccades. The architecture of this model allows to highlight the fact that the saccadic suppression would be a consequence of efficient Bayesian state estimation, in such way that the noise in the motor command would reduce the importance given to the visual sensory information.

In the present work, the inverse statement has been tested experimentally to challenge the hypothesis, since the model is also built such that increasing the weight of the sensory feedback in the estimation would impair the outcome and disturb the motor command. Participants underwent a task during which their perception was enhanced during saccades, modulating the intensity of the suppression, in order to measure the outcome on the saccadic movement.

A control task was added to verify results from a former work, confirming that with an increased sensory input, the behaviour of the saccades differs from the regular main sequence. Those results support the idea that saccadic suppression could originate from optimal sensorimotor estimation. However, those results must be seen as a plausible explanation in the framework of sensorimotor control, and the link with physical neural circuits needs to be further investigated.

Contents

Chapter 1

Introduction

1.1 What is saccadic suppression?

While looking at a scenery, we perceive a clear, large and stable image of what lies in front of us. This can look rather simple, but in reality, our eyes perform numerous rapid movements to form the picture perceived by our brain. Indeed, the retina is covered with neurons called photo-receptors, which can be either cones or rods. The cones are the cells that are responsible for the vision of colors and the visual acuity, and are located mainly in the fovea. While the rods are responsible for our vision in dark surrounding, and are located around the fovea, as shown in Fig.1.1. This results in humans only seeing precisely the part of the scenery that is projected in the fovea. The consequence of the eyes moving unconsciously to project the points of interests towards this location are rapid eye movements, also called saccades [1].

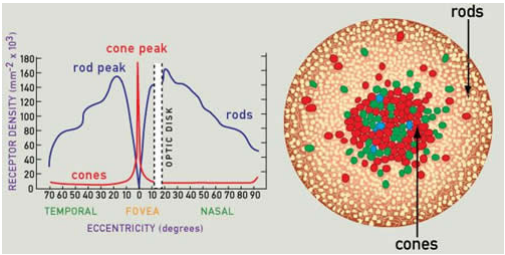

Figure 1.1: Distribution of cones and rods on the surface of retina [2]

So while looking at a scenery, the eyes just send a set of high resolution snapshots to the brain and three interesting events happen: First, we are able to know the

location of every snapshots, even though they are just sent through the optic nerve, allowing humans to have a clear understanding of the scene. Second, the brain is able to make the difference between motion of the image on the retina, and the motion of elements in the scenery. And third, during the eyes movements, the vision is blurred and the acuity is far worse than that of the snapshots [3]. The present work focuses on this last phenomenon called saccadic suppression.

Saccadic suppression has been first described a long time ago, in 1898, by Erdmann and Dodge [4]. And since then, we are still learning about it, as techniques improve with time [5]. It has been shown that during this phenomenon, the brain selectively blocks the visual signal during and around the eye movements, resulting in a blurred image, and in a great reduction of motion detection. This consequence on motion detection has been reviewed by J. Ross and colleagues [6], in regard with spatial frequency and luminance of the presented moving gratings, in order to show links with the visual pathways. J. Ross also made a review in 2001 about the visual perception during saccades, adding that saccades would change the apparent position of the target, causing displacement and compression of the image [7]. The suppression begins about 75 ms before the eye movement onset, is maximal at the onset, and outlasts it for about 50 ms [8].

1.2 Vision pathways and neural correlates of the suppression

While talking about vision, it is interesting to address the neurological pathways that are used. Indeed, it is essential to understand how vision works in order to understand where the saccadic suppression could take place in the brain. While looking at our scenery, the visual information is sent by the photoreceptors to the ganglion cells that form the optic nerve. This first information flux ends in the lateral geniculate nucleus (LGN), located in the posterior part of the thalamus. The LGN can be separated in two main structures: the parvocellular (P), and magnocellular (M) layers, in which end the ganglion cells that were already differenciated between P and M in the retina. Magnocellular layers acquire their information from rods, are colorblind and specialized in motion detection, while parvocellular layers process information originating from cones, have slower conduction and are specialized in color differentiation and details [9]. Those two kinds of layers will be useful to understand the separation of the information treatment at the end of the primary visual pathway. The visual information will then be sent from the LGN towards the primary visual cortex (V1) located in the occipital lobe. Once in the V1, the information is transmitted through two different pathways: the ventral and dorsal streams. The ventral pathway goes through the visual areas 2 (V2) and 4 (V4), and

finishes its course in the inferior temporal cortex [10]. The ventral stream is known as the parvocellular pathway, or the "What" pathway, since it is linked with form and color perception, and objects recognition. The dorsal pathway, on the other hand, goes through visual area 6 (V6), and the medial (superior) temporal (MT) and visual area 5 (V5), up to the lateral parietal cortex (IPL and SPL). This stream also goes by the magnocellular pathway, since the magnocellular neurons follow the same path. It is also called the "Where/How" pathway, since it is associated with movement, objects location and saccades guiding. Those pathways are illustrated in Fig.1.2(a).

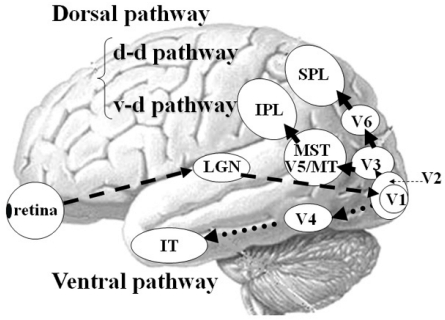

(a) Illustration of the dorsal and ventral pathways. They both begin in the retina, and pass through the LGN and V1/V2. The ventral pathway then goes through V4 and finishes in the inferior temporal cortex. The dorsal pathway goes to the parietal cortex, passing through medial, medial superior temporal area, and V5 [10].

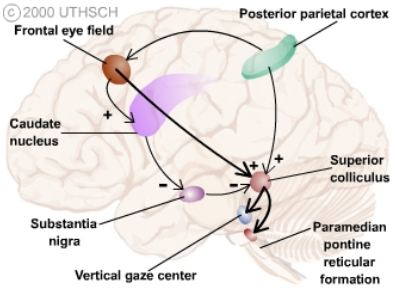

(b) Illustration of the pathways responsible for the saccadic eye movements. The signal is send from the parietal cortex towards the frontal eye field and the superior colliculus, and the to the motoneurons responsible for the eye movements [11].

Figure 1.2: Pathways describing the visual input (a) and eye movement output (b)

Once the image sent to our brain has sufficiently been analysed, the brain is ready to analyse another point of interest in the scenery, leading to a new saccadic eye movement. The information about the former snapshot comes from the posterior parietal cortex, and is sent both to the frontal eye field, and the superior colliculus (SC). The frontal eye field is known for managing voluntary saccades, while the SC has a role in reflex orienting saccades. Those two structures then send information to other sites, resulting in the activation of abducens, oculomotor and trochlear motor neurons, initiating the eye movement and controlling the saccade. More details are available in Fig.1.2(b) [11].

As for the saccadic suppression, it appears to happen mainly in the magnocellular stream, which conveys fast and colorblind information, such as stimuli with low spatial frequency and high temporal frequency [12]. Techniques such as Positron Emission Tomography (PET), blood oxygen level dependant (BOLD) fRMI, and others, allowed to shed some light on the areas linked with saccadic suppression.

Electrophysiological measures allowed to show that saccades affect single cells visual responses in the LGN, the middle temporal (MT), the middle superior temporal (MST), and the intraparietal (IP) areas (IPL and SPL in Fig.1.2). And psychophysical data showed that suppression is stronger with stimulus that activate mainly the magnocellular neurons, and thus that suppression could happen in the dorsal stream. fRMI imaging supports this latter hypothesis: suppression of the BOLD signal has been found V1, V2, quaternary visual area (V4), septenary visual cortex (V7), and in the human motion complex (hMT+), which plays a role in movement detection. These observations lead to think that saccadic suppression operates mainly in the dorsal stream, and is an extra-retinal mechanism, which means it is operated when the information has already gone through the retina [13].

1.3 Famous hypotheses for the suppression mechanism

There are still major uncertainties regarding the reason why this phenomenon happens. In this section, two famous hypotheses are reviewed, although other less supported theories exist: The first theory, posited among others by E. Castet and his colleagues, regards saccadic suppression as a mechanical consequence of the retinal movement. The second one defends that the suppression happens in order to stabilize the perception, and is supported among others by R. Wurtz. Both theories are plausible but meet difficulties that will be discussed here.

- The first theory, supported by Castet and his team, states that saccadic suppression doesn't have a functional role and is a consequence of mechanical shear force on the photoreceptors. Indeed, the acceleration due to the movement bends the photoreceptors and this prevents the light rays to enter directly, which would explain the perisaccadic suppression timings. This is known as the Stiles-Crawford effect and results in a decrease of the captured luminance, leading to a visual adaptation decrease, and thus to a loss of sensitivity in the magnocellular pathway. They support that saccadic suppression is a consequence of what happens on the retina level and causes changes in visual processing [14].

The weaknesses of this hypothesis have been highlighted in the response of Ross, Burr and team to the letter of Castet in "Trends in neurosciences" [15]. For example, the Stiles-Crawford effect only affects cones and not rods, however, saccadic suppression also happens in darker environments in which rods play a role. If the suppression phenomenon was located on the retina, information from all kinds of neurons would be affected. However, it is known that the saccadic suppression effect is restricted on luminance-modulated low frequency stimuli. Furthermore, as explained above, the suppression has been demonstrated as an extra-retinal phenomenon by imaging techniques, and was also highlighted using TMS [16]. Finally, because of the vitreous humor, the shear forces that were thought to be maximal at the beginning and end of saccades are damped, which is not consistent with the saccadic suppression being maximal at the movement onset.

- The second hypothesis, supported by Wurtz in his review [3], claims that saccadic suppression could be one of the mechanisms allowing visual stability of the field of view. Stability could be an element of response for the role of saccadic suppression, making up for the disruptions of the visual inputs caused by saccades, but it cannot explain the whole purpose of the phenomenon. Indeed, some characteristics of the saccadic suppression are not explained by the purpose of stability.

  First, the timing of the suppression does not match with the stability hypothesis. As stated before, the decrease of sensitivity begins about 75 ms before, and is maximal at the saccadic onset. The amount of discarded visual information during the phenomenon is bigger than what would be expected if the only goal was to maintain stability during the eye movement, which is not an expected behavior, knowing the efficiency of the human brain.

  And second, it has been shown that the sensitivity decrease is not the same between an "active" saccade, when eyes follow a target jump, and a "passive" saccade, when the background image moves at the same velocity the image would on the retina during an "active" saccade but with the eyes remaining stationary [17].

1.4 Model of saccadic movements control

In this section, a model F. Crevecoeur and K.P. Kording [18] created with the aim of observing the saccadic system with a control point of view, will be presented. The present work aims at reproducing experimentally results that have been simulated thanks to this model; this will be explained in details below. The model is built

under certain assumptions that lead to the following features. First, contrary to what has often been assumed, saccadic eye movements cannot be seen as ballistic (meaning the final state of the eye plant could be predicted by the initial motor input), because they are affected by an efference copy called the corollary discharge (CD) and are updated during the displacement; this must be translated into a closed-loop design. Second, even if the vision is blurred during the eye movement, we still see something because the sensory inflow is still there, bringing the need for a sensory feedback in the model. Also, this feedback needs to be delayed since ≈ 100 ms are passing by between a stimulus and the saccadic response.

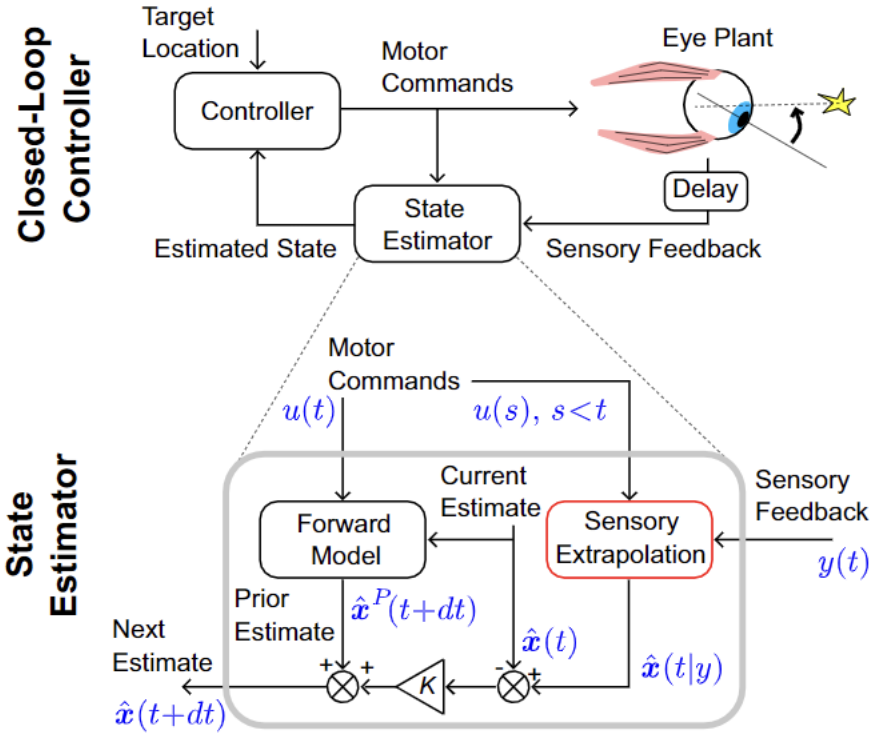

Figure 1.3: Structure of the saccade control model of Crevecoeur and Kording [18]. Top: Schema of the closed-loop controller, with the features resulting from the made assumptions. Bottom: Focus on the state estimator. The sensory extrapolation gives a corrected estimation of the state, taking the previous motor commands and the delayed sensory feedback as input. The forward model gives an estimation of the state at the next step, taking the current motor command and estimate as input. The Kalman filtering gives an optimal estimation of the next state, that is sent to the LQG controller, to update the motor command.

The model is illustrated in Fig.1.3, and is described in this paragraph. The model

controller is Linear-Quadratic-Gaussian (LQG). It takes the sensory feedback and the corollary discharge as input, and outputs the motor commands sent to the eye plant, which is a second order model. The most interesting feature of this model, regarding saccadic suppression, is the state estimator. It allows to correct the trajectory of the eyes and is composed of two main elements: a forward model and a sensory extrapolation element.

The forward model updates the current state estimation, it takes the estimated state of the eye plant and the motor command as input and outputs the prior estimated state of the next time step. The sensory extrapolation element allows to have an extrapolated state estimation. Indeed, since the sensory feedback is delayed due to the information travel time, we cannot use it as such and it must be extrapolated to be compared with the prediction of the forward model. In other words, the sensory extrapolation will give a correct state estimation, but it cannot be used as such since, because of the delay, it is too late. And the forward model gives a estimated state of the next time step that is on time to change the next command in the controller, but that is "ill"-estimated, since it does not take the sensory feedback into account. The model will use those two estimations: a correct state estimation that is too late, and an inaccurate state estimation that is on time, to build a correct state estimation of the next step. The last calculation done by the model is to put the two information together: $\hat{x}(t+dt) = \hat{x}^P(t+dt) + K(t)(\hat{x}(t) - \hat{x}(t|y))$, using a Kalman filter. The Kalman weight will have an influence on the importance of the feedback on the next step estimation, allowing to send the final next step estimated state to the controller, and to update the motor command.

1.4.1 Link between motor noise and saccadic suppression

Knowing the components of this saccades control model, it is possible to link a certain consequence of signals interactions with saccadic suppression. The ocular muscles generate signal dependent noise, which induces a higher variance in the model control signal. Because of the delay, the brain is not able to modulate or suppress this noise, leading the extrapolation error computed in the state estimator to be larger. This can be summarized by stating that the sensory signal becomes uncertain because of the noise produced by the motor command. This variance induced by the control signal varies with time, is enhanced during the eye movement, and has an influence on the Kalman weight. Indeed, Kalman filtering is a technique used to have an accurate estimation of the state of an object, using knowledge about its current and prior whereabouts. The update of the estimated time steps involves an algorithm in several parts in which the optimal Kalman gain depends on the inverse covariance of the previous estimate. Indeed here, variance in motor

command is inversely proportional to the Kalman weight of the eye position and according to F. Crevecoeur and K.P Kording, this can be related to the saccadic suppression phenomenon. The predictions of the model show that the sensory feedback should be lower during the window of the suppression in order to optimally estimate the state of the eye, and this specific phenomenon can be paralleled with the saccadic suppression.

When testing the model and comparing the results of the simulations with real data, they showed that the model captures saccadic, but also smooth pursuit movement behavior. They also observed that the timings of the weight reduction are comparable with the timings of saccadic suppression. Moreover, the model predicted that the suppression should begin prior to the movement onset, be maximal around its beginning, and scale with its amplitude.

1.5 Previous investigations and contributions of the present work

Since it is complex to test experimentally if the sensory perception is impaired by the motor signal, F.Crevecoeur and K.C. Kording suggest to demonstrate the inverse statement: showing that the noise in muscle command disturbs the perception could be the same as showing that increasing the sensory input also increases the variance of the motor command. Indeed, if the Kalman weight is increased by a enhanced focus on perception, the estimation of the next state should be suboptimal, leading to more variable motor commands. This corollary hypothesis has been tested in Benjamin Roberfroid's Master's thesis [19]. He increased the importance of the sensory signal by asking participants to focus on stimuli flashed during saccades. Participants had to detect the stimuli's tilt they perceived, this enabled him to have a score in order to quantify the weight of the sensory information. He also could show that the endpoint error increased with time, which goes along with the hypothesis. However, those results did not allow to conclude whether the increasing endpoint error is indeed a consequence of the increasing sensory weight, or if the participants just planned to stop the saccades earlier to see the stimuli better.

The aim of this thesis is to try to reproduce the results of B. Roberfroid, but also to add a control trials task to the experiment, allowing to compare the trials where the saccades were disturbed by the tilted stimuli, with control trials with no stimuli, in which the targets would jump towards the points where most of the disturbed trials of B. Roberfroid ended.

The results of those experiments will allow, in the first place, to reproduce the

previous results of B. Roberfroid, showing first evidence of a "sensory input-dependant" motor command. More importantly, comparing the control to the disturbed trials will allow to prove the results are not biased by voluntary stopped saccades, and that the motor commands were sub-optimally estimated because of the enhanced visual signal. Those results will give evidence that, as implied by Crevecoeur and Kording from their model, saccadic suppression is due to efficient sensorimotor estimation.

Chapter 2

Materials and methods

2.1 Equipment

During the experiment, the participant's dominant eye has been tracked by the Eyelink 1000 eye tracker from SR Research (Ontario) [20], that sampled the positions in the horizontal and vertical axis at 1000 Hz. The device was placed on a table and a headrest ensured head stability.

The tasks were displayed on a screen in a dark room by a Barco cine 8 projector from the other side of the room, with a resolution of 800x600 pixels.

The scripts used during the experiment were written and ran in MATLAB, using the 7.5.0 R2007B version. The PsychToolBox (3.0.8) and CosyGraphics (3-beta78) toolboxes have been used. Additionally, the participants could interact thanks to a keyboard placed right in front of them.

2.2 Participants

Fifteen participants, including 9 females, aged between 20 and 25 years old (mean of 22.9333 and standard deviation of 1.8310 years), took part in the experiment. The dominant eye of 13 participants was the right eye, three participants were astigmatic and myopic, one was only myopic, and one was only astigmatic. Their impairment were corrected by lenses, except for two whose myopia was low, including one whose myopia only affected his non-dominant eye.

2.3 Protocol and display

The experiment can be sequenced in three main tasks: the control task, the training task, and the perturbation task.

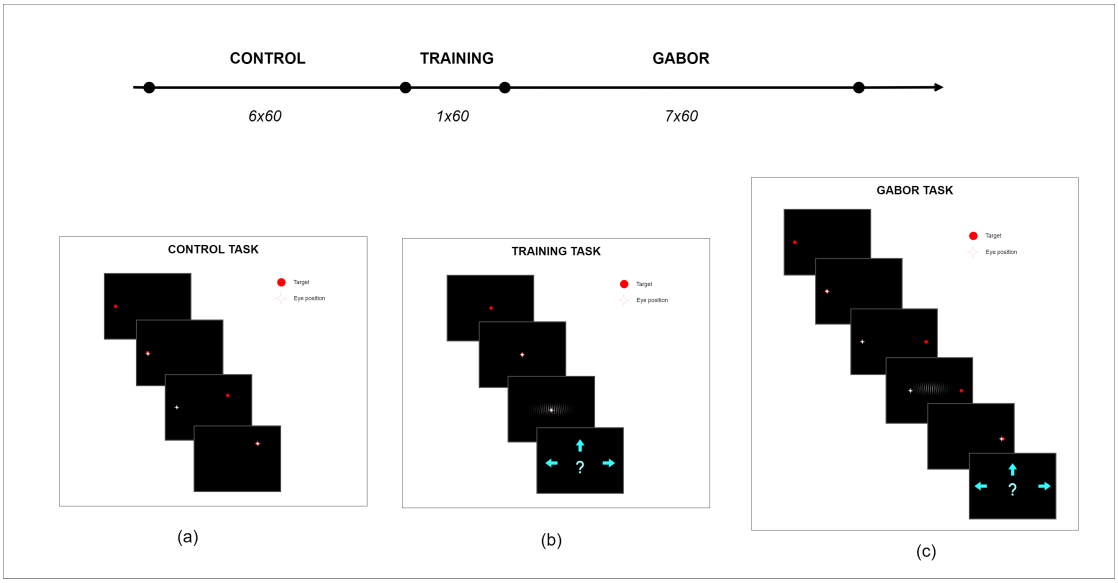

Figure 2.1: (a) The control trials began with the subjects fixing the initial target during the defined timing, the target then jumped toward one of the twenty control targets (6 blocs of 60 trials, 18 trials to each of the 20 targets in total). (b) The training trials started with a fixation target at the center of the screen to draw the paticipant's attention to the location where the stimulus would appear. One of the three possible tilted Gabor patch then appeared and the participant had to answer with the tilt she/he perceived (one bloc of 60 trials). (c) The Gabor trials started with a fixation target that made a twenty degrees jump. Once the beginning of the saccade was detected, the Gabor patch was flashed, and the question about the tilt was asked again to the participants (7 blocs of 60 trials).

2.3.1 Control task

This first part of the experiment was designed in 6 blocks of 60 trials. For each trials, the participant had to perform a saccade beginning at [-10°,0°] and ending at targets randomly chosen among twenty targets, so that each of these twenty targets would appear 3 times in every block. Based on the dataset of B. Roberfroid, nineteen of those twenty targets were chosen as the centers of the neighborhoods where at least 80% of the disturbed saccades ended. The distribution of those trials is illustrated in Fig. 2.2(a). The last target was located at [10°,0°] to generate an

unperturbed saccade amplitude of 20° comparable with Gabor task target jump amplitude (see Fig.2.2(b) for the final location of the control targets).

During those trials, the targets were displayed on a black screen as red circles with diameter of 8 pixels. The fixation target was displayed between one to three seconds (the fixation timing was chosen randomly to avoid anticipation from the participants), then it disappeared and one of the twenty targets appeared for 1.1 seconds, as shown in Fig.2.1(a). At the end of this control part, the participant reached 18 times towards each target.

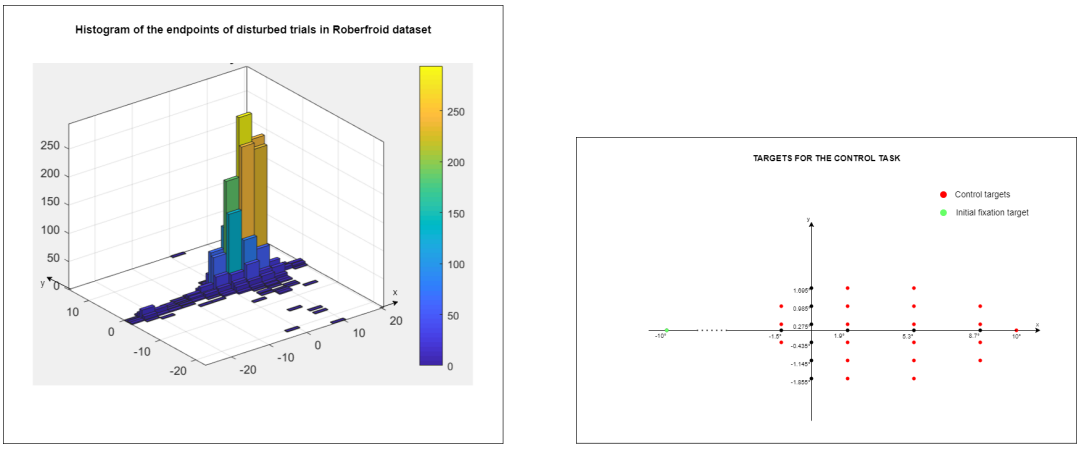

(a) (b)

Figure 2.2: (a) Histogram of the disturbed saccades' endpoints from B. Roberfroid's dataset. The histogram has 14 × 54 bins, each covering a rectangle of (3.4° × 0.71°). (b) The 19 control targets represent the centers of the 19 bins that cover the vast majority (80.43%) of Roberfroid's saccades endpoints. The 20^{th} target lies at (10°,0°) to be comparable with the disturbed task of this thesis.

2.3.2 Training task

After the control task, the participants were introduced to the stimulus. This part was made of one block of 60 trials during which a stimulus was flashed for 10 ms just in front of the participant, from three different possible tilt angles with a uniform probability, so that each stimulus was flashed twenty times. The stimulus was a Gabor patch and its three different tilts were -5°,0°, and 5° as shown in Fig.2.3. The Gaussian patch had the following parameters: a size of 250 × 300 pixels, covering a large region of the field of view. The spatial frequency was 0.1 cycle per pixel and the Gaussian envelope was designed in such a way that the width was five times greater than the height. The participants had about 1.5

seconds to press a key corresponding to the angle tilt they thought they perceived, as in Fig.2.1(b).

Figure 2.3: From left to right: -5°, 0°, and 5° possible tilt angles of the Gabor patches.

2.3.3 Perturbation task or Gabor task

After the training, the participant had to perform a 20° saccade, during which she/he was disturbed by a Gabor patch. At the beginning, the participant had to stare a first target placed at [-10°,0°] for during between 1 to 3 seconds, before the target jumped towards [10°,0°]. Once the program detected the beginning of the saccade, the Gabor patch was flashed, and the participants were asked to once more press the key corresponding to the orientation of the stimulus they perceived. The steps are described in Fig.2.1(c). The participants performed this task for 7 blocs of 60 trials. This high number of trials was used to provide the opportunity to try to increase the sensory information weight along the blocks, and, thus to potentially observe an evolution.

In order to detect the beginning of a saccade, the program computed the second order upstream difference of the positions to obtain the velocity:

$$v(t) = \frac{3x(t) - 4(x(t-h) + x(t-2h))}{2h}$$

where h = 1 ms was the time step. The chosen speed threshold to detect the beginning of the saccade was set to a velocity greater than the absolute value of 150 degrees/second during 4 ms.

2.4 Data processing

Before being analysed, the data was preprocessed according to the following steps:

- Prior to the data acquisition, a first online calibration of the Eyelink was made for each participant. It allowed to scale the amplitude of the eye positions the camera recorded, which depend on the physical characteristics of the face and the positioning. This online calibration was done prior to any recording.

- Before looking at the data, the eye position signals were filtered with a zero-phase digital Butterworth low-pass filter of fourth order, with a cut-off frequency of 50 Hz.
- Then, a first offline calibration was applied. At the beginning of each block, the participant was asked to look at nine green points, forming a calibration cross: [±10°,0°], [±20°,0°], [0°,±7°], [0°,±11°], and [0°,0°]. All the eye positions of the trials in the bloc were rescaled and translated in the right values.
- After the filtering and the first calibrations, the saccades were isolated from the whole recording of each trials. Another computation of the velocity and another threshold were used. The velocity profile of the trials was computed with a central numerical derivative of second order [21]:

$$v(t) = \frac{x(t+h) - x(t-h)}{2h}$$

  with h = 1 ms. The saccade was detected with such a velocity threshold that a saccade began when the velocity rose higher than 10°/s and stopped when the velocity came back down under 10°/s.
- The data was then calibrated a third time in such a way that the mean start point of each bloc (control and Gabor blocs) would be at [-10°,0°].

The saccades were then sorted out in order for each included trials to meet the following requirements. Those requirements are named from R1 to R4 to allow a further analyses of the percentage of trials inclusion:

- R1: Regardless of the task, the saccade was made in the direction of the target and there was no blink during the saccade. For the Gabor task, the following requirement was added: the program had to detect the beginning of the saccade to ensure that the Gabor patch was displayed during the trial.
- R2: Regardless of the task, the saccade was made in the direction of the target, there was no blink during the saccade and, the gaze did not move more than 0.5 horizontal degrees during the 200 ms preceding the target jump
- R3: Regardless of the task, the saccade was made between 70ms and 500ms after the target jump.
- R4: For the control task, the saccade did not undershoot for less than 90% of the expected endpoint [22].

The percentages of included trials for each task and for each participant are available in Table5.1 (see appendices).

For the control task, it should be noted that, on average, 83.15 % of the performed saccades were kept for further analyes, and that 87.53% of them ended up in the designed grid (defined below). This means that 72,78 % of all the control saccades were used for the comparison with the Gabor trials.

For the Gabor task, on average 84% of the trials were kept, among which 92.49 % ended up in the grid. This large percentage reflects that the grid was well chosen and gives a first intuition that this Gabor task could give results comparable with those of B. Roberfroid. On average 77.69 % of the total Gabor trials were thus be used for the comparison with the control trials. It can also be noted that the average score of the training trials was 96.89 %, which was significantly higher than the average score of the kept trials in the Gabor task. This confirmed that the Gabor patch displayed during the training task was clearly visible when there was no eye movement, and that a phenomenon, which is likely to be the saccadic suppression, happened during the Gabor task.

2.5 Statistical analyses

Two types of statistical tests were used for the analyses.

2.5.1 Paired t-tests

Paired t-tests were used to compare observation between the first and last blocs of the Gabor tasks in the first part of the analyses. They were also used to compare the variance of measures between Gabor and control trials in the second part of the results chapter. This test decides if the mean of the first group of sample is significantly different from the mean of the second samples group; it is if $p - value < \alpha = 0.05$, and it assumes a normal distribution of the differences between the pairs of data [23]. In this thesis, one-tailed paired t-tests were used to test if the groups were different toward a direction. For example:

$$H_0 : \mu_{group1} = \mu_{group2} \tag{2.1}$$

$$H_1 : \mu_{group1} < or > \mu_{group2} \tag{2.2}$$

2.5.2 Linear mixed models

Linear mixed models (LMM) are an extension of linear models that take fixed and random effects into account. It allowed, here, to fit a linear regression on what was analysed, that sees the effects within a participant and between participants. The regression follows the model:

$$y = \mathbf{X} \cdot \beta + \mathbf{Z} \cdot \mathbf{u} + \epsilon \tag{2.3}$$

where X is the matrix of the predictor of the fixed variables, for example the trial number, of the grid box in which a trial ends. The β are a column of the associated regression coefficients, also containing an intercept. The matrix Z contains the random variables, for example the participant. The column u gives the complement of the random effect to the regression coefficients. ϵ is the column of residuals [24]. The intercept and slope of the regression are defined significant if the $p - value < \alpha = 0.05$. To compute those linear mixed models, the MATLAB function fitlme() was used. The analyses described in the results follow these models:

$$Scores \approx 1 + Bloc + (1|Participant) \tag{2.4}$$

$$Endpointerror \approx 1 + Trial + (1|Participant) \tag{2.5}$$

$$SDEndpointerror \approx 1 + Trial + (1|Participant) \tag{2.6}$$

$$Peakvelocity \approx 1 + Trial + (1|Participant) \tag{2.7}$$

$$Duration \approx 1 + Trial + (1|Participant) \tag{2.8}$$

$$SI \approx 1 + Trial + (1|Participant) \tag{2.9}$$

These are presented in the Wilkinson notation, where 1 represents the intercept, $Bloc$ and $Trials$ are the predictor variables that represent the fixed effects (giving a slope and an intercept), and $(1|Participant)$ means that the random effect only has an effect on the intercept of the presented models.

2.6 Definition of quantities and grid

- **The endpoint error** was defined as positive if the trial amplitude was less than 20°, and as negative if more than 20°.
- **The standard deviation of the endpoint error** was computed sliding over 10 trials.
- **The peak velocity** was defined as the maximal horizontal velocity during the saccade.
- **The symmetry index (SI)** quantifying the skewness was such that:

  $$SI = \frac{D_a}{D}$$

  where D is the duration of the saccade, and D_a is the duration of the eyes acceleration, as illustrated in Fig.2.4. It means that in a velocity profile where $SI < 0.5$, the acceleration lasts less time than the deceleration of the

eyes and that the velocity profile is "symmetrical" if $SI = 0.5$. However, this definition of symmetry has limitations since it only takes the timings of peak velocities and saccade durations into account, and ignores the behavior of the curve.

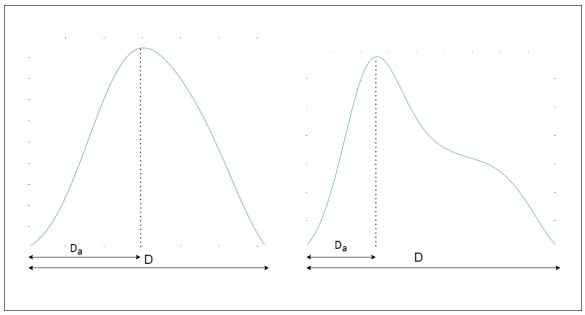

Figure 2.4: Two velocity profiles for illustration purpose

- **The number of inflexion points** ($\#IP$) of the velocity profiles was defined as the number of zeros of their derivatives. For example, the velocity profile on the left in Fig.2.4 has two inflection points, while the profile on the right has four. This allowed to differentiate classic velocity profiles from odd ones.
- As reminder, **the interquartile range** is a dispersion measure defined by the difference between the 75^{th} and the 25^{th} percentiles of the data. This quantity was used in the second part of the results chapter.

Definition of the grid In order to evaluate if the choice of the control targets was relevant, and to be able to compare the control trials with the Gabor trials, a grid was defined. It was defined similarly to the two-dimension bins of the histogram made with Roberfroid's dataset. The grid is composed of rectangles in which the centers are the 19 control targets. The 19 rectangles have a width of 3.4° horizontally, and a height of 0.71° vertically, as shown in Fig.2.5(a). Every box of the grid was given a number to facilitate further analyses.

Definition of boxes of interest (BOI) During the second part of the result chapter, the grid boxes, in which most of the trials end, will be taken into consideration. To do so, a box is defined as of interest, provided that at least 15 Gabor trials of a specific participant end in it. The occurrence of each box for every participant is rendered in Fig.2.5(b).

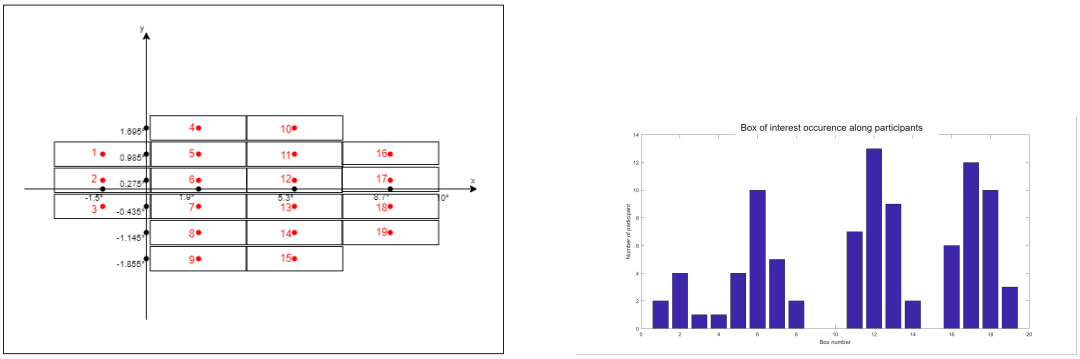

(a) (b)

Figure 2.5: (a) Grid defined based on Roberfroid's dataset of Gabor trials. It is used to compare Gabor and control trials. (b) Occurrence of each grid box of interest (BOI) for every participant, a BOI being defined as a grid box in which 15 trials or more end.

Chapter 3

Results

As reminder, the experiment was composed of two main tasks. During the first task, the participants were asked to perform control trials towards targets ending at strategic locations, thereby allowing a future comparison with the trials of the second task. For the second task, the participants were asked to perform seven blocs of 20° horizontal saccades, during which a tilted stimulus was flashed. They were then given a score depending on their perception of the stimuli; this task is called the Gabor task. The details are available in the Materials and methods chapter.

In this chapter, for the purpose of clarity, the results concerning control trials will always be displayed in red, while the Gabor trials will be displayed in blue.

The Fig.3.1 represents the trajectories (a) and the velocity profiles (b) of exemplar participants, and helps to discriminate the analyses in two parts. Indeed, looking at these trajectories (a), the amplitudes of the Gabor saccades seem to decrease along the blocs. This supports that time is a major factor that changes the behavior of the saccades and could give the opportunity to the participants to change variables in their internal control model. The first part of this chapter will thus focus on the changes along the trials and the blocs for the Gabor task. Those results will be comparable with those of B. Roberfroid.

Then, the velocity profiles (b) show a substantial difference between the Gabor and the control trials that aimed for a 20° jump, since the Gabor trials seem more variable than the controls. This leads to the idea of comparing the 20° amplitude control saccades with the Gabor trials, but also of comparing control and Gabor trials that end their course in the same grid box (see Materials and methods). This comparison using endpoint box will help differentiating whether, the Gabor saccades are willingly stopped before the final target or whether it could be a consequence

of sensorimotor inferences. The analyses between control and Gabor trials will be reviewed in the second part of this chapter, and are the main contribution of this work.

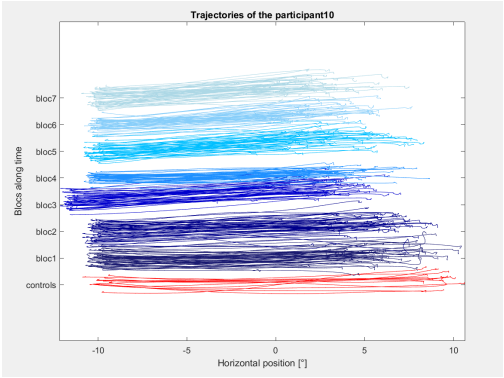

(a) Saccades trajectories

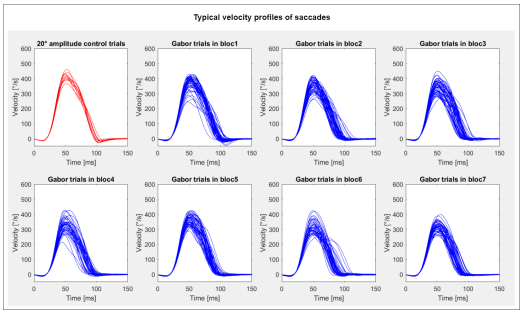

(b) The velocity profiles are aligned on the beginning of the saccades.

Figure 3.1: Trajectories of participant 10 (a) and velocity profiles of the participant 7 (b) for the 20° control saccades (in red) and for each Gabor blocs (in blue). The plots begin 20 ms prior, and end 150 ms posterior to each saccades. Trajectories show a decrease of amplitude along the blocs, while the velocity profiles show more variance for Gabor trials than for the controls.

3.1 Analysis of saccades across time

As explained above, this section will focus on observing the Gabor saccades along the time. Several measures are analysed, such as the scores, the endpoint errors and the associated variance, the peak velocities and saccade durations, as well as the symmetry indexes.

3.1.1 Scores

The score of the participants along time is a good indicator of whether their focus on the Gabor patch increases, whether the weight of the sensory input in the control model increases, and also whether the suppression can be modified with time. Indeed, Fig.3.2(a) and (b) shows that, the scores increase along the blocs of the Gabor task, this increase is supported by the LMM in equation (2.4) ($b = 3.0808$, $t_{103} = 7.4359$, $p < 10^{-6}$) and by the paired t-test ($p = 4.55 \times 10^{-6}$,$t_{14} = -4.9068$)

3.1.2 Endpoint errors

A sharp increase of the mean endpoint error can be noticed during the first trials (associated with bloc1), followed by a much slower increase for the rest of the task, see Fig.3.2(c) and (d). This was confirmed by the LMM in equation (2.5) ($b = 3.538 \times 10^{-3}$, $t_{5325} = 11.914$, $p < 10^{-6}$) and by the paired t-test ($p = 9.6 \times 10^{-3}$, $t_{14} = -2.6478$).

This increase of endpoint error over time supports the hypothesis that the motor command could be suboptimally optimized. Indeed, the focus increase in participants would cause the increase in sensory feedback, as suggested by the model. However, showing this hypothesis also requires showing that the saccades are not the same between the control and the Gabor trials, this will be investigated in the second part of this chapter.

3.1.3 Endpoint error variances

In their article [18], Crevecoeur and Kording suggested that the saccades would vary more if the sensory input increases.

First of all, the standard deviation of the horizontal endpoint errors is shown in Fig.3.2(e). The average mean of the standard deviation is smaller in the bloc1 (60 firsts trials) than in the bloc7 (60 lasts trials), which would support the aforementioned hypothesis. However, the associated LMM in equation (2.6) did not confirm this result and the slope is slight ($b = 9.2 \times 10^{-5}$, $t_{6248} = 1.0557$, $p = 0.291$)

To further investigate the evolution of the endpoint error variance, as the LMM proved to be non-significant, the endpoint errors in 2D (x and y-axis) were displayed for the bloc1 and bloc7, then a principal components analysis was carried out for each cluster (see Fig.3.2(f)). The area of the ellipse in bloc1 and bloc7 was then computed to form an idea of the ellipse dispersion, which gives a measure of the variance (see Fig.3.2(g)). A paired t-test showed that, on average, the endpoint errors were more dispersed in the first bloc than in the last ($p = 0.03$, $t_{14} = 2.046$), which shows that the variance of the endpoint error decreases with time, as opposed to the first prediction.

3.1.4 Peak velocities

The average peak velocity decreases rapidly in the first trials and slowly for the rest of the task, resulting in an average velocity drop of $\approx$ 80°/s between the beginning and the end. This trend can be seen in Fig.3.3(a) and (b), and has been verified with the LMM in equation (2.7) ($b = -7.831 \times 10^{-2}$, $t_{5325} = -11.735$, $p < 10^{-6}$) and a paired t-test ($p = 1.01 \times 10^{-2}$, $t_{14} = 2.046$).

This result might, however, be a simple consequence of an adaptation of the internal control called repetition suppression, and will be discussed later.

3.1.5 Symmetry indexes/skewness

The last feature investigated is the skewness of the velocity profiles in the x-axis.

The symmetry indexes are plotted in grey in Fig.3.3(c); the SI decreases rapidly in the first trials and more slowly for the rest of the task, the SI also seem to vary more after the first bloc, see Fig.3.3(c) and (d).

This trend is confirmed by the LMM in equation (2.9) ($b = -1.8421 \times 10^{-5}$, $t_{5325} = -4.4364$, $p = 9.33 \times 10^{-6}$), but not by the paired t-test ($p = 0.2284$, $t_{14} = 0.7651$). The trend supporting the SI's decrease can, nonetheless, still be accepted since the result to keep in mind is the large decrease observed at the beginning of the task, and this is this sharp decrease that shows the tendency in the linear mixed model, which is also more precise than the paired t-test.

In summary, a few things can be observed about the results concerning the Gabor trials along time. The scores of the participants increase in time, highlighting a learning process as well as the fact that the saccadic suppression phenomenon could be modified, allowing a better sensory feedback during the movement. The endpoint errors increase along time, resulting in an increasingly smaller amplitude. This could mean that the motor control is impaired by the increasing sensory feedback, and will be verified in the second results section by comparing those trials with the controls. Those two firsts results are consistent with those B. Roberfroid observed. Moreover, the variance of the endpoint error seems to decrease with time, which could contradict Crevecoeur and Kording's prediction. This will be discussed later. The peak velocities also tend to decrease with time, which could either be linked with an adaptation phenomenon, or with the fact that saccades amplitudes decreases with time, this will also be further discussed in this work. Finally, the SI decreases with time, which means that the velocity profiles' skewness increases, this might be related with abnormal velocity profiles containing multiple peaks.

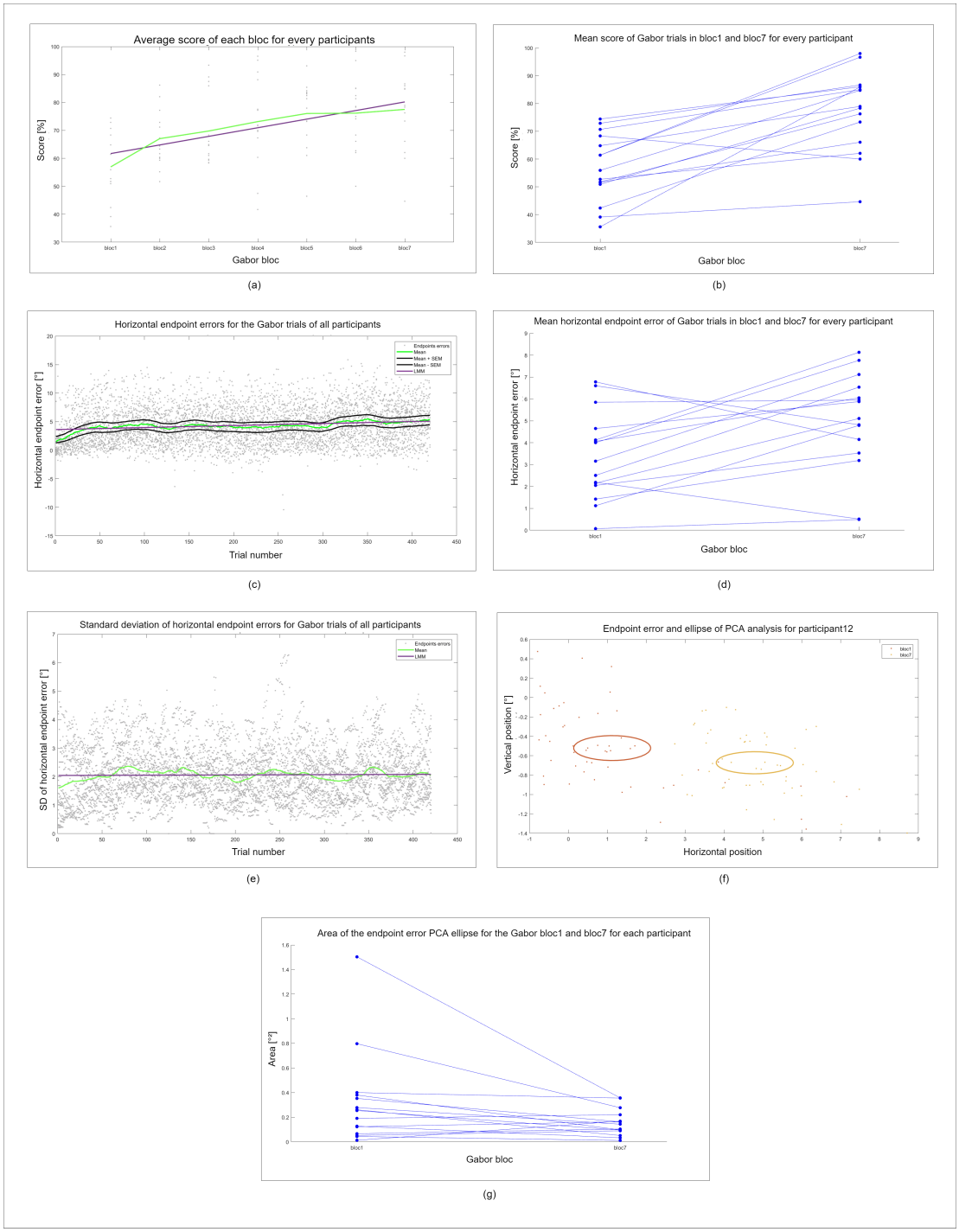

Figure 3.2: (a) Scores of the participants for each bloc, average in green, and LMM in purple. (b) Focus on the scores of each participant for the bloc1 and bloc7. A significant increase over time is noticed. (c) Horizontal endpoint error for each trials of each participant, the green mean is a sliding average of the mean per trials, over 20 trials, for the standard error of the mean in black (SEM), the sliding SD over 20 trials of the mean per trial has been used. The same computing have been done for all the similar plots of this panel. (d) Mean endpoint error of each participant for bloc1 and bloc7. A significant increase over time is noticed. (e) Standard deviation of the horizontal endpoint error. (f) Endpoint error in x and y, and ellipses of PCA for bloc1 and bloc7 of participant 12 as example. (g) Area of PCA ellipses in [$^{\circ 2}$] in bloc1 vs bloc7 for each participant, this gives another measure of the variability of the endpoint errors.

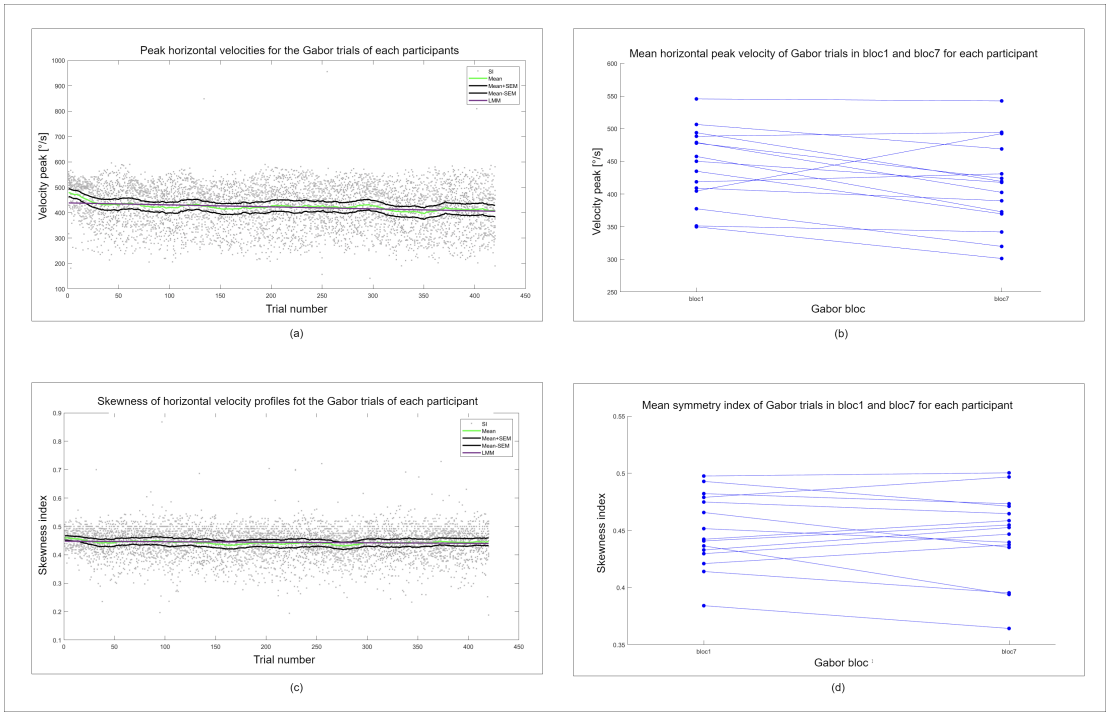

Figure 3.3: (a) Peak velocity for all trials of every participant. (b) focus on the mean peak velocity in bloc1 and bloc7 for each participant. A significant decrease over time is noticed. (c) Symmetry indexes along every trials. (d) Mean SI for bloc1 and bloc7 for each participant. A decrease over time is noticed.

3.2 Comparaison between the control and Gabor tasks

A last analysis ensuring that the Gabor task impairs the motor control of saccade was done by comparing all Gabor trials with the horizontal 20° control trials. As seen in Fig.3.4, the average endpoint errors, such as their standard deviations, for each participant, is larger for Gabor trials than for controls.

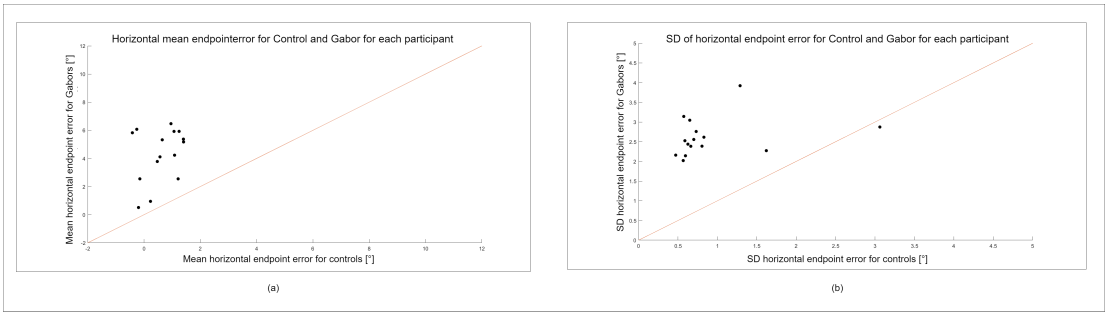

Figure 3.4: Comparison of the horizontal endpoint errors for the 20° control trials and the Gabor trials for each participant. (a) Mean endpoint error. (b) Standard deviation of the endpoint error.

For the rest of the analyses, trials ending in the same grid box will be compared, it will help differentiating if the Gabor saccades are willingly stopped before the final target or if it is maybe a consequence of sensorimotor inferences. Some results will be highlighted by comparing trials from boxes across the entire grid, and others by comparing box of interests, excluding location where few trials end up.

3.2.1 General differentiation between control and Gabor trials

In order to get a first idea of the differences between control and Gabor trials, the correlation of the velocity profiles has been computed. To do so, for each grid box, the mean control velocity profile has been computed (black line in Fig.3.5(a) and (b)). Then, in each box, the correlations of each control profiles (red lines in Fig.3.5(a)) with the mean control profile have been averaged. Which gives one control correlation per box. The same calculation was done to get a box averaged correlation of each Gabor trial profile (blue lines in Fig.3.5(b)) with the mean control profile. Finally, the correlations across every boxes have been averaged, providing a single control correlation and Gabor correlation per participant. The grids of Gabor and control velocity profiles for each participant are available in the annexes.

This allows to show in Fig.3.5(c) that qualitatively, there is a difference between the Gabor and velocity profiles, a paired t-test showed that the correlation of controls trials is larger than the correlation of the Gabor trials with the mean control profile ($p = 1.02 \times 10^{-2}$, $t_{14} = 2.6167$). This result justifies the relevance of the further analyses.

Also, according to the theory behind the model, the increase of sensory feedback

should affect the motor command of the saccades. The increase of sensory feedback can be translated in a score increase, while the suboptimal optimization of the motor command can be translated in a Gabor correlation smaller in absolute terms but also smaller than the control correlation. This idea was investigated in Fig.3.5(d). In other words, the normalized correlation is expected to decrease for better scores. The fitted linear regression shows the opposite effect, but is not significant ($b = 2.9 \times 10^{-2}$, $t_{13} = 0.409$, $p = 0.689$).

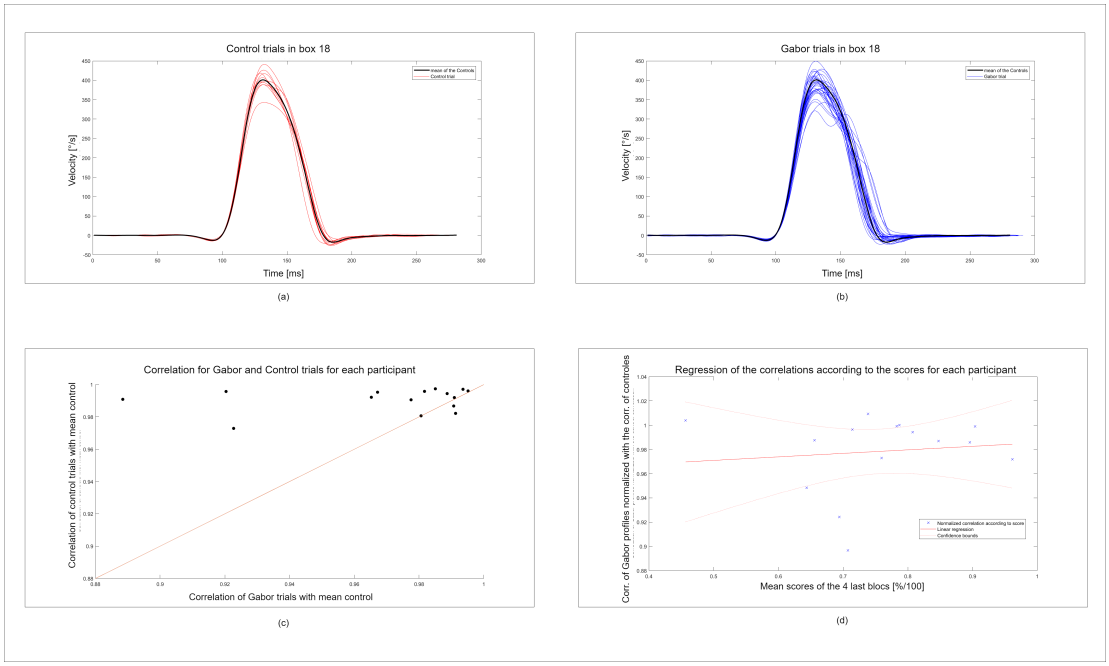

Figure 3.5: (a) Example of control velocity profiles in a box, with the average profile in black. (b) Example of Gabor velocity profiles in the same box. (c) For each participant, the correlation of the controls with the mean control profile and the correlation of the Gabor profiles with the mean control profile are scattered. (d) The Gabor correlations normalized by the control correlations are scattered for each participant depending on their scores for the last four blocs. Discarding the three first blocs allowed to ensure the score variation due to the learning did not affect the result. The slope of the regression is positive (but not significant), as opposed to what was expected, certainly due to too little data and other reasons which will be discussed further in Chapter 4.

3.2.2 Comparison of Gabor and control data across all the grid boxes

For the analyses in this section, the medians of measured quantities in each grid box were averaged across the boxes, resulting in one control and one Gabor quantity for each participant.

Median peak velocity: If averaged over every grid boxes, the median peak velocity is larger for Gabor trials than for the control trials ($p = 3.95 \times 10^{-2}$, $t_{14} = -1.894$), this is depicted in Fig.3.6(a). A hypothesis explaining this result would be that since the motor commands for the Gabor trials are first coded to be 20° saccades (even if they end before, due to the displayed stimulus), their peak velocities would be larger than the control saccades coded to end in boxes requiring smaller amplitudes.

Median duration: As seen in Fig.3.6(b), the averaged median durations of Gabor trials are larger than those of the control trials ($p = 1.04 \times 10^{-2}$, $t_{14} = -2.6031$).

Median symmetry indexes: The averaged median SI are larger, thus, the velocity profiles are more symmetrical for the control trials, showing an enhanced skewness for the Gabor trials ($p = 1.56 \times 10^{-2}$, $t_{14} = 2.393$).

The same analyses have been done by isolating the boxes of interest (defined in Materials and methods) from the boxes in which few trials ended. The results were less emphasized and no more significant although the trends stayed the same, as if the results were diluted. However, this could mean that the measured effects in Gabor trials differ more when they end in "outliers" boxes, and even if those are less frequent, this could be seen as a big enough difference and will be discussed in the next chapter.

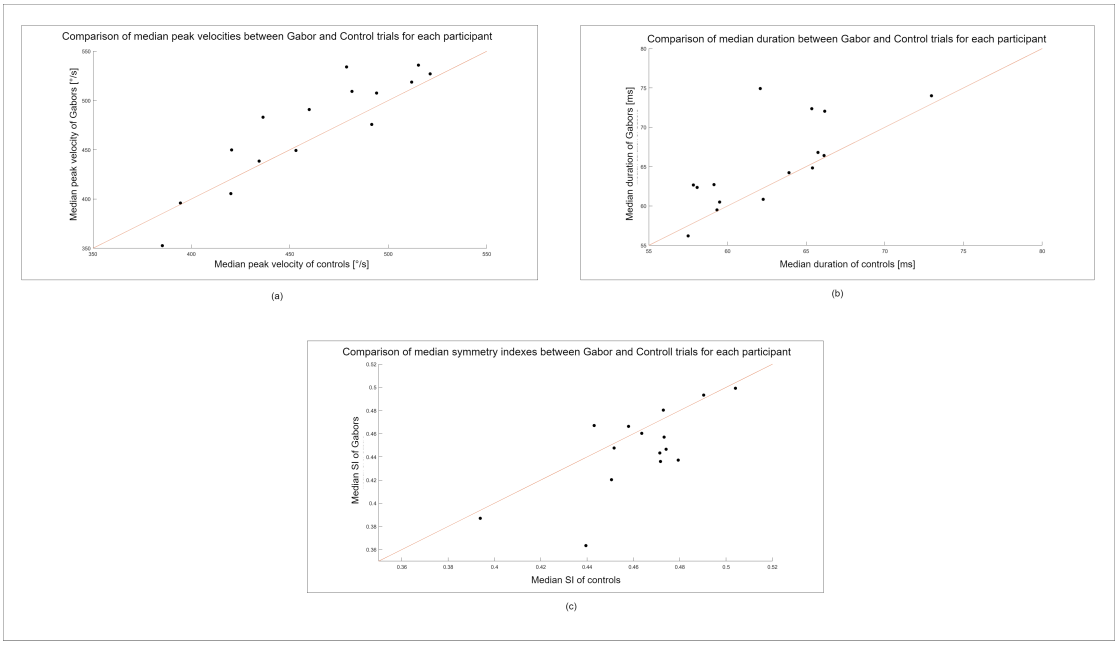

Figure 3.6: Illustrations of the comparisons across all the boxes: (a) Average comparison per box of median velocity peaks for the Gabor and control trials. The velocity peaks are larger for the Gabor trials than for the controls. (b) The same analysis was done for saccades durations, and Gabor trials tend to last longer than the controls. (c) The control trials are more symmetrical than the Gabor trials.

3.2.3 Variance of the trials between Gabor and control task in box of interest

By looking at Fig.3.7, it can be noticed that the Gabor trials (in blue) are more variable than the control trials (in red) that end in the same grid box. In this section, the interquartile range (IQR) of the velocity peaks, the symmetry indexes, and the number of inflexion points in each box of interest will be analysed.

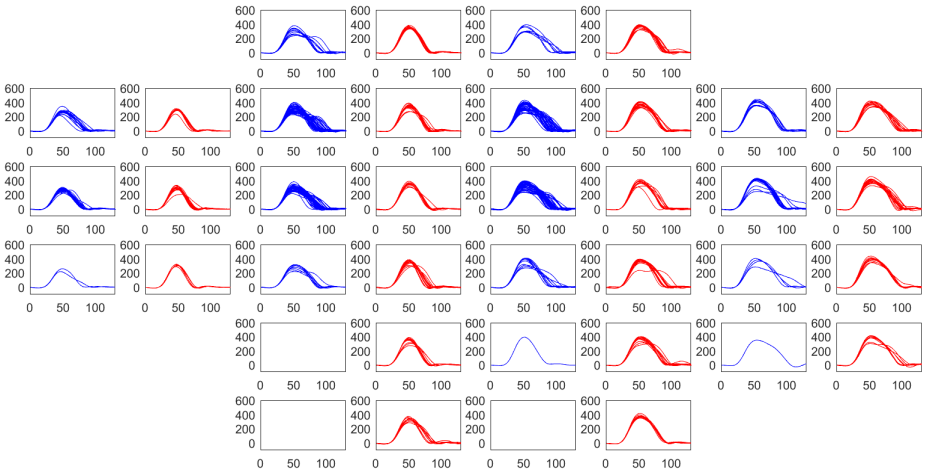

Figure 3.7: Participant 10 taken as example: Velocity profiles across the grid of the Gabor and Control tasks. For every grid box, the figure shows the Gabor trials in blue and the control trials in red. For this participant, a higher variance in velocity peak and number of inflexion points can be noticed for the Gabor trials, this difference led to the analyses described in this section.

For each box of interest, the IQR has been computed (75^{th} percentile value $-$ 25^{th} percentile value) for both the Gabor and control trials. The averages IQR across the boxes for each participant are available in Fig.3.9. The grid boxes where too little saccades ended were not taken into account because they would have had the same weight in the averages, and would not give an appropriate measure of the trials variability.

IQR of the velocity peaks: The velocity peaks are more variable for the Gabor trials than for the controls ($p = 2.9 \times 10^{-3}$, $t_{14} = 3.248$), as seen in Fig.3.9(a). This can be explained by the trials profiles that do not follow the known main sequence of velocity profiles according to amplitude (main sequence illustrated in Fig.3.8), since lots of Gabor trials velocity profiles have multiple peaks, due to the perturbation.

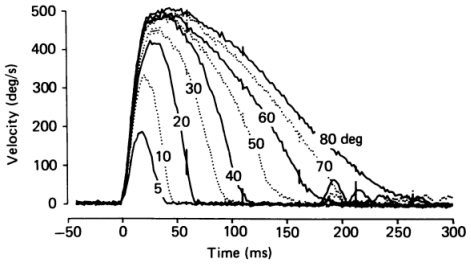

Figure 3.8: Stereotypical velocity profiles of normal saccades, known as the main sequence. [25]

IQR of the symmetry indexes: From previous analyses, control trials seem to have a SI near 0.5, while the Gabor trials have smaller SI, since their profiles with multiple peaks tend to reach their peak velocity sooner. The analyses of the IQR of the SI show a trend in which the Gabor trials are more variable than the controls (Fig.3.9(b)), but this was not significant ($p = 7.47 \times 10^{-2}$, $t_{14} = 1.526$).

IQR of the number of inflexion points: The number of inflexion points in the velocity profiles can be linked with the skewness, and analysing the IQR is therefore relevant to differentiate Gabor and controls trials. The trend shows that the IQR of #IP is larger for Gabor than control trials, but is not significant when only the boxes of interest are used ($p = 0.176$, $t_{14} = 0.963$). The same trend became significant when the analysis was done over the whole grid ($p = 3.61 \times 10^{-2}$, $t_{14} = 1.3445$). This difference in the results (Fig.3.9 (c) and (d)) makes it essential to question the way the trials are analysed.

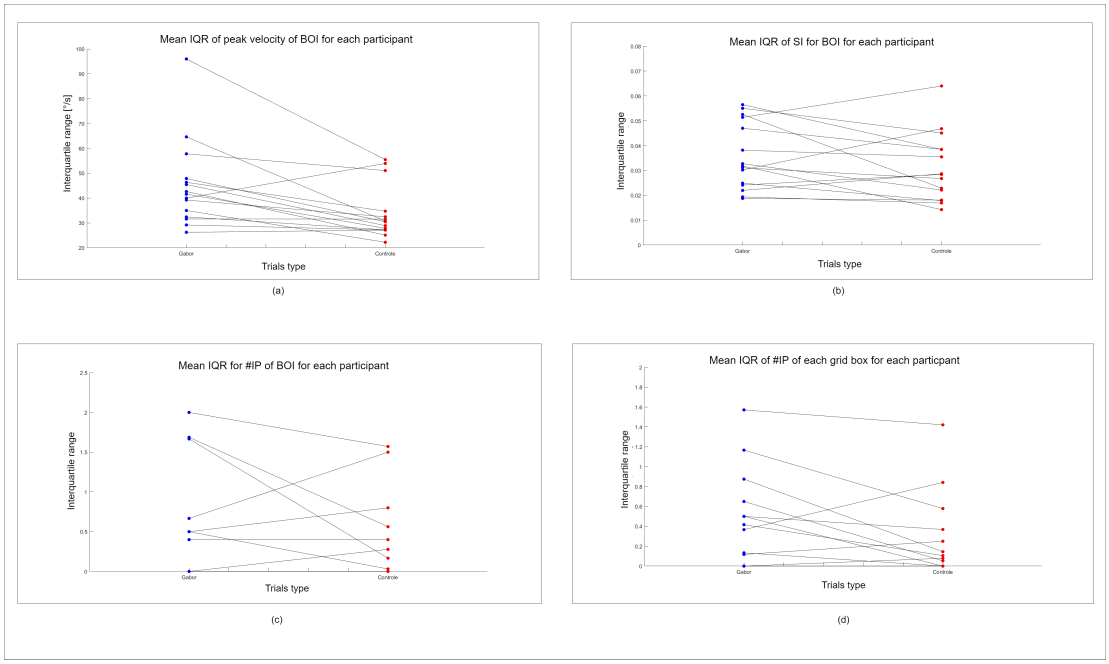

Figure 3.9: Difference of the boxes averaged interquartile ranges between Gabor and control trials for: (a) The velocity peaks across boxes of interest (significantly larger in Gabor trials). (b) The SI across the boxes of interest (non-significantly larger in Gabor trials). (c) The number of inflexion point in the velocity profile across the boxes of interest (non-significantly larger in Gabor trials) and (d) across all the grid (significantly larger in Gabor trials).

Chapter 4

Discussion and conclusion

The aim of this thesis was to investigate whether, based on the presented model, the saccadic suppression phenomenon is a consequence of sensorimotor estimation. Indeed, the conclusion drawn from the model is that the partial suppression of visual information during the saccade is due to the noise brought by the motor command. By looking at the model, one can conclude that increasing the visual feedback during the saccade would impair the quality of the motor command sent to the eye muscles. This second proposition was verified experimentally, in order to validate the conclusion about the saccadic suppression origin that is drawn from the model.

This work can be summarized in two steps: First, the possible impact of the visual information on the saccadic motor control was verified, and second, a comparison was made between a task for which the visual information was enhanced during the saccades and a classic target jump control task.

4.1 Main results of the Gabor task analysis along time

The measurements made during the first step have been analysed across time to be able to notice a change in the trials outcome.

First, the scores of the Gabor task were poorer than in the training task, which, thus, validates that saccadic suppression happened during the experiment. Furthermore, the scores got improved across time, showing a learning curve from the participants and an increased quality of the sensory visual feedback, meaning that the intensity of saccadic suppression can be modulated. As already demonstrated in the work of

B. Roberfroid, the horizontal endpoint error of the saccades increased with time, resulting in a decreasing movement amplitude. The second part of the analyses is required to ensure that the increasing endpoint error is the consequence of an impaired motor command and not an intentional stop to get a better view at the stimulus.

Contrary to what was predicted by Crevecoeur and Kording, with the statistical tests used in this work, the variance of the participant's endpoint errors did not increase with time. The reason for this behaviour is uncertain; it might have been distorted by the analysing methods. Indeed, as for other measures, the mean endpoint error variance across all participants changes (and increases) mostly during the first bloc, and this short time variation could maybe be enough to validate the prediction. However, this has to be taken with caution, since the participant-wise endpoint error variance clearly decreases between the beginning and end of the Gabor task. Although the variance in endpoint did not increase, the variance of the velocity peaks increased along time, and mainly during the first bloc (see Fig.5.1 in Annexes). This can be seen as a consequence of a less efficient motor command and enhanced focus on the sensory information; indeed, more and more saccades have a velocity peak not corresponding to that of a 20° amplitude saccade. This could also explain the multiple peaks in the velocity profiles: to have a better sensory information while still approaching a 20° displacement, the saccade would be done in several steps, while not stopping, which implies several lower velocity peaks.

Another result to bear in mind is the decrease of peak velocity across time. An obvious explanation, supporting the model on which the experiment is based, would be that the velocity peaks are decreasing due to the decrease of the saccades amplitude with time. However, this still has to be discussed since a similar result has already been demonstrated in another context. Indeed, an experiment including repeated horizontal control saccades made by Chen-Harris et al. [26] showed a decrease of velocity peak with time, which they explained as a decrease of motivational state of neural origin, called "repetition suppression" (see Fig.4.1). However, two elements are challenging this explanation. First, the duration of their saccades, correlated with the peak velocities, increased with time, while the saccades durations of this work's experiment decrease with time. This difference cannot however discard the repetition suppression phenomenon idea, since our decreasing durations could simply be linked with the decrease in saccades amplitude. Second, it is difficult to state whether the drop of peak velocity along time is the same in the two experiments. Indeed, in Chen-Harris experiment, there was a large number of 15° amplitude saccades, while our data only contains eighteen 20° control saccades per participant, which makes a comparison of the peak velocity drops impossible. A solution to verify whether the velocity peaks decrease is due to

the repetitions or to the consequence of the suboptimal estimation, would simply be to add more 20° saccades jump trials in the control task.

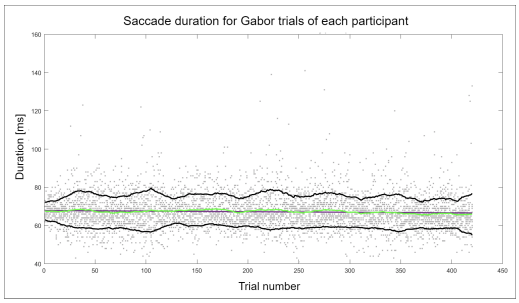

(a)

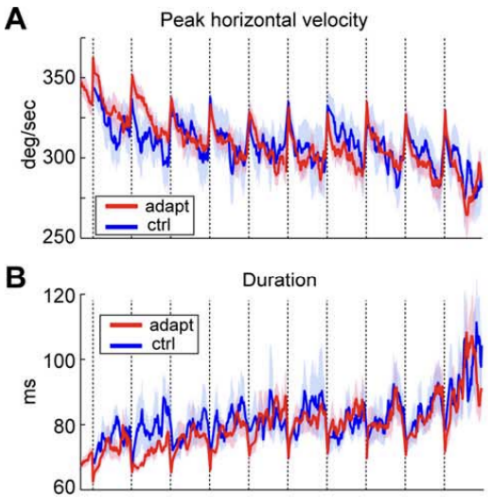

(b)

Figure 4.1: (a) Duration of the saccades along the Gabor trials. (b) Results (in blue) showing repetition suppression in the experiment of Chen-Harris et al. [26]

4.2 Main results of the comparison between the Gabor and control trials

The second step consisted in comparing disturbed and control tasks trials that ended around the same location, in order to verify that the change of behaviour was not intentional in the Gabor task.

A first analysis comparing the correlation between the Gabor and control trials with the mean of control trials showed a quantitative general difference between the velocity profiles in the two tasks, encouraging further analyses.

Based on the model, an obvious prediction would be to state that if the score improved, the correlation of the Gabor velocity profiles with the mean control velocity profile would decrease. Indeed, an improvement of the score indicates an enhanced visual feedback, and would cause more variability in the motor command leading to disturbed velocity profiles of saccades. Contrary to what was expected, the analyses showed a correlation increasing with the scores. It is important to realize that showing a link between those two measures is difficult: While the score only depends on three different possible answers, the correlation of the Gabor

velocity profiles with the control depends on many different parameters. Indeed, it is difficult to differentiate the two sorts of saccades ending near the location of the stimulus, having different motor intents.

The first kind are the saccades are those, which are voluntarily stopped on the stimulus to perceive it clearly. Those saccades, while having a large correlation with the controls since the movement is not disturbed, would give a good score. The second kind are the saccades expected by the experiment, stopped unintentionally far from the 20° target because of the suboptimal motor command, resulting in a good score because of the good visual feedback, but with a low correlation with the controls since it was disturbed. A way to avoid this confusion would be to make this correlation according to score analysis, but only by keeping trials that ended far enough from the stimulus. There would still be the drawbacks that a lot of data would be discarded, and that such a strategy would only focus on the velocity profiles and not on the endpoints, making this analysis possibly biased and to use with caution.

After the analyses of correlation between velocity profiles, comparison between Gabor and controls for the median quantities in boxes for all the grid boxes were done. It was found that the peak velocities and durations were higher for the Gabor trials, and that their velocity profiles were less symmetrical than the classic undisturbed saccades. In addition, the number of inflexion points in the velocity profiles were more variable for Gabor trials. These results were diluted when looked at only for the boxes of interest where most of the Gabor trials ended, as if only a few trials from boxes in which just a few saccades ended influenced the overall results. Moreover, analyses focusing on the difference of variance of the velocity profiles between Gabor and control tasks were done over the boxes of interest. They showed a larger variance of the velocity peaks, and a larger variance of the symmetry indexes (almost significant). Those results confirmed that there exists a difference between Gabor and control trials, and therefore validates the experiment.

In other words, the difference of results between the analyses for all boxes and for boxes of interest helped to show some differences between the two sorts of trials. For example, it was noticed that peak velocities and durations were different for less frequent box locations, by having allocated the same weight to every box. Thus, this highlighted the fact that trials that end up in rarely solicited locations are maybe those that are the more disturbed by the stimulus.

Considering another perspective, it is difficult to aggregate the data across every box and every subject since there is a risk of concluding that a trend does not exist. For example, if a trend does exist for each participant, but not in the same locations, it might be invisible. This is what happened with the analyses of the

quantity variability: there was no difference between Gabor and controls for the peak velocity and symmetry index variances when the analyses were carried out across the whole grid, it was only detected when solely checking the boxes of interest.

However, this way of analysing the results raises questions. Is it sufficient to show there exists differences between Gabor and controls at some locations, that are maybe not the same for each participant? It could be acceptable to show that effects can sometimes depend on the boxes where fewer saccades ended because those might be the boxes where the trials were the most disturbed, even if the disturbances were less frequent. And from the other perspective, even though some effects seem to be attenuated when the less solicited boxes are removed, it does not imply that there is no effect or that it is less marked. It could only mean that they are not generalized in the same location for every participants. The results of both analytical techniques appear acceptable, provided they are taken with caution.

4.3 Limitations and further directions

Normal saccades are known for their almost symmetrical velocity profiles. However, unusual velocity profiles have been observed in several control trials. These profiles contain multiple velocity peaks, which makes them look like some of the Gabor trials (this behaviour can be seen in Fig.5.3(a)). This observation is troubling and no explanation has been found to explain it. This could be due to an acquisition problem, or to an unnoticed behaviour of the participants, since only two of the fifteen participants experienced them, as seen in Fig.4.2). Those strange velocity profiles might have minimized the average differences between the Gabor and control trials. Fortunately, this does not change the conclusion of the results, since it makes the search for differences more challenging. However, those participants should maybe have been removed from the data analyses, since it is uncertain if those uncanny profiles were also present for no apparent reason on their Gabor trials.

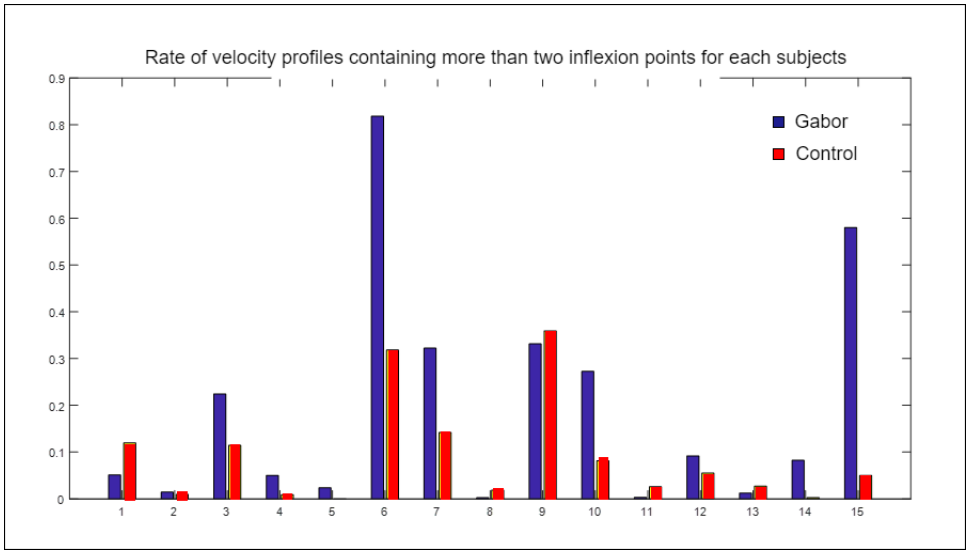

Figure 4.2: Rate of velocity profiles containing more than two points of inflexion. Those types of velocity profiles are uncanny when present in the control trials, as seen for participants 6 and 9.

A second limitation of this work was observed during the data acquisition. Participants reported that they perceived the stimulus angle as more tilted due to the direction of the saccades. More precisely, they saw the stimulus as rotated clockwise. This was not documented but they had a tendency to perceive the 5° tilted patch as vertical, and the 0° tilt patch as the -5° tilt, prompting them to answer the -5° and 0° keys more often than the 5° answer. This could have modified the real scores, since some participants, that noticed their perception was skewed, corrected their answers accordingly, while the others did not correct it albeit they also noticed the distortion. A possible improvement if the experiment had to be reproduced, would be to perform the saccades in the two direction while asking the participants not to change their answering strategy during the acquisition.

Third, questions were raised concerning the most correct method for aggregating the data across the endpoint locations and participants. No clear response was found since the two methods used gave slightly different results that still went toward the same direction. However, there exists another analysing method that could bypass this conceptual problem of method selection. Indeed, during the analyses aiming at differentiating the Gabor and control trials, linear mixed models could have been used again. The idea would be to characterize the trials by their location as a fixed effect, and to keep the participant dependent behaviour as a random effect. For example, the model could take the position in x and y of the center of the grid box in which the trial ended up, or take the angle α and distance

d between the start position of the saccade and the position of endpoint box:

$$y = \beta_0 + \beta_1 \times \alpha + \beta_2 \times d + \epsilon_{participant} + residual \tag{4.1}$$

Building such models for Gabor and control trials could allow to observe the impact of the grid boxes locations on the measured y quantities, while taking every trials into account for the analysis, by comparing the two linear regressions of Gabor and control tasks. However, the differences between the regressions would be difficult to interpret since it would depict the evolution of the quantities along the boxes as predictor variables.

Also, even though the data acquisition gave 420 Gabor and 360 control trials for each participant (not counting the exclusion during the pre-processing), this amount of data is maybe too small to show clear tendencies in variance analyses. Stronger results could have been acquired with a dataset containing more than fifteen participants.

And finally, this work supports the claim that Crevecoeur and Kording's model shows important evidences that the saccadic suppression is, indeed, due to efficient sensorimotor estimation. The next step would be to show that this is not only true for the model, but also for our actual brain. Linking a model to reality is complex. The model is an abstraction facilitating the comprehension of a concept, while the brain is a complex physical system. It is thus challenging to link control, signal integration, estimation and filtering to specific locations in the brain. For example, the model mixes motor and sensory inputs for the sensory extrapolation, whereas sensory input and motor output pathways seem to be separated in the brain. However, there is an element giving hope to try. Indeed, simulations on the model have also shown to replicate the behaviour of smooth pursuit similarly to real physiological data [18]. Articles have also shown that saccadic and smooth pursuit eye movements could share the same sensorimotor process in the brain [27][28][29], but also that the visual system shares resources between perception and movement [30]. This gives one more reason to go further and try to link the model with neural correlates, for instance by searching for regions that use information from both the motor-dependent noise and corollary discharge.

4.4 Conclusion

The goal of this work was firstly to reproduce the results of B. Roberfroid, but mainly to ensure that the experiment made sense by finding out if the Gabor trials were different from the control trials. The first part was successfully confirmed, showing an improvement of the score and an increase in endpoint error along time,

next to revealing other varying quantities. In a second time, it has been shown that the Gabor and control trials are significantly different, for some measures across the whole plane, and for other measures, about specific locations depending on participants. However, it is still complicated to harmonize these results, even if they go towards the same direction.

On a bigger picture, the confirmed differences between Gabor and control trials allow to validate that the Gabor task really disturbed the participants and that they did not willingly behave to stop their eye movements sooner to better see the stimulus. The improvement of the score across time shows that the weight on the sensory input increases with time, and the disturbed endpoint errors and velocity profiles lead to think that the motor commands were sub-optimally computed. Those observations confirm Crevecoeur and Kording's predictions about the "inverse" use of the model they built, confirming that, on a dynamical control model point of view, the saccadic suppression phenomenon is due to the optimal estimation of sensorimotor information.

Chapter 5

Appendices

5.1 Main trials information

	CONTROL					GABOR					
Participant	% kept	% R1 and % R2	% R3	% R4	% kept grid	% kept	% R1 and % R2	% R3	% kept grid	% score kept	% train score
1	85.83	2.22	3.61	8.33	92.33	92.86	5	2.14	98.46	68.47	98.33
2	85.56	2.78	3.89	7.78	70.78	82.86	5.48	11.67	98.85	68.53	96.67
3	53.33	1.67	1.94	43.06	83.33	85.95	3.1	10.95	83.10	69.42	93.33
4	94.17	5.83	0	0	83.13	90	5.24	4.76	99.47	61.12	95
5	98.61	1.39	0	0	92.39	71.43	10.95	17.62	76.67	62.55	98.33
6	85.56	14.4	0	0	95.78	87.86	10.71	1.43	95.66	61.33	98.33
7	90	9.72	0	0.28	94.44	85.71	12.62	1.67	99.44	83.47	100
8	88.33	6.67	1.39	3.61	83.02	92.62	3.1	4.29	99.23	70.94	98.33
9	57.22	19.72	10	13.06	84.47	78.33	11.19	10.48	99.09	71.76	98.33
10	85	0	2.5	12.5	84.31	89.05	6.43	4.52	99.47	70.33	96.67
11	85.56	8.61	3.33	2.5	85.39	76.9	20.95	2.14	92.57	49.73	86.67
12	80.56	2.22	5.28	11.94	91.03	82.86	6.19	10.95	95.98	89.37	96.67
13	61.11	1.94	5	31.91	94.09	57.62	35.95	6.43	98.76	86.73	98.33
14	96.39	3.61	0	0	88.47	89.52	9.05	1.43	97.07	74.27	98.33
15	100	0	0	0	90	96.43	3.57	0	53.58	76.18	100
TOT	83.15	5.39	2.46	9	87.53	84	9.97	6.03	92.49	70.95	96.89

Table 5.1: Summary of the inclusion/exclusion of the trials, their presence in the grid, and the score associated. The percentages of included trials for each task for each participant are available in the columns "% kept". The columns "% R1 and R2", "% R3", and "% R4" contain the percentage of trials discarded because they did not meet the corresponding requirements. The columns "% kept grid" of the table contain the percentages of included saccades that end in the grid. In the Gabor part of the table, the column "% score kept " contains the percentages of the participant's correct answers to the included Gabor trials. And finally, the column "% train score" contains the percentage of the participant's correct answers to the training task, which is the task where the Gabor patches were flashed while the eye position stays steady.

5.2 Velocity peak variance

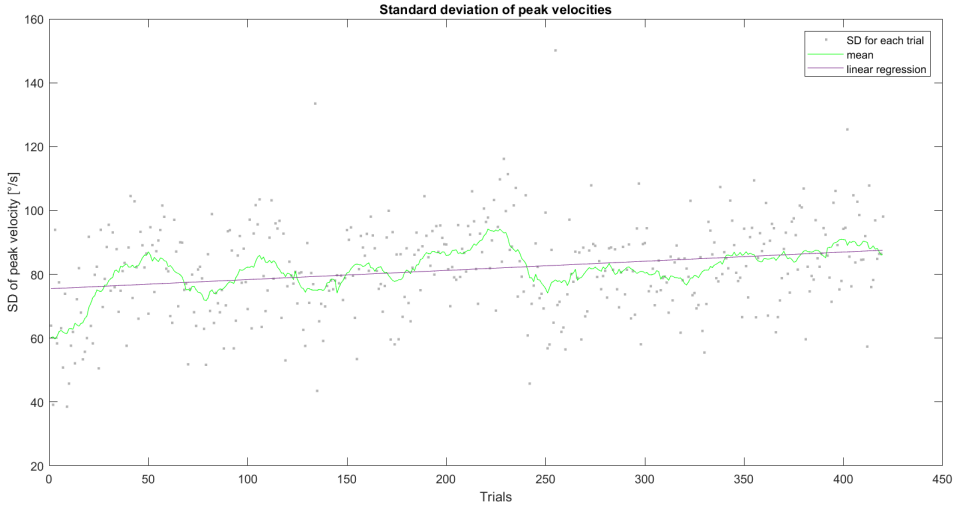

Figure 5.1: Standard deviation of the peak velocities along the trials

5.3 Velocity peaks across the grid for every participant

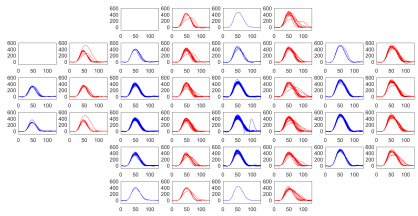

(a) Participant 1

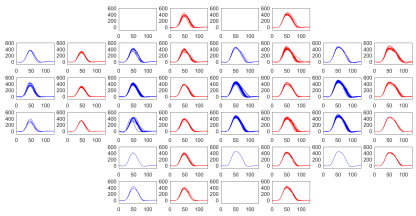

(b) Participant 2

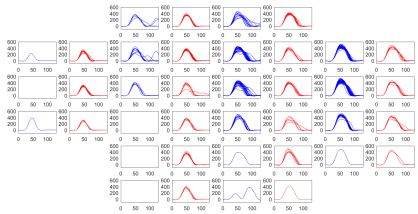

(c) Participant 3

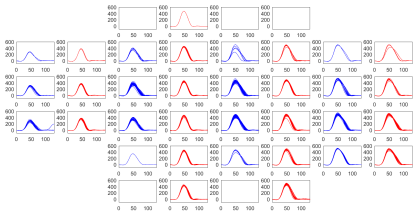

(d) Participant 4

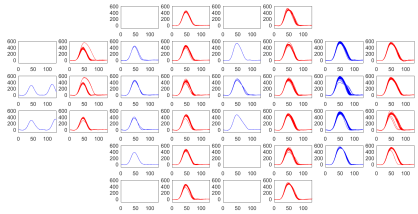

(e) Participant 5

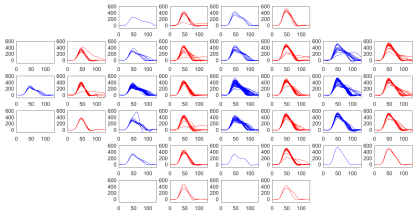

(f) Participant 6

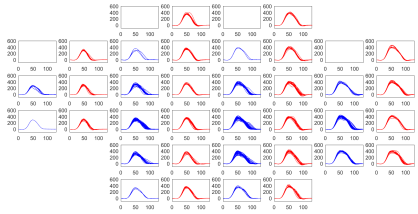

(g) Participant 7

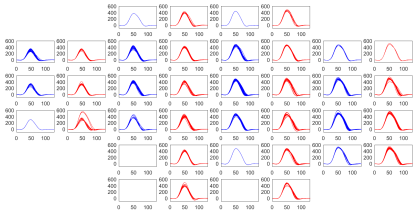

(h) Participant 8

Figure 5.2: Velocity profiles in the grid for all participants: Gabor in blue and control in red.

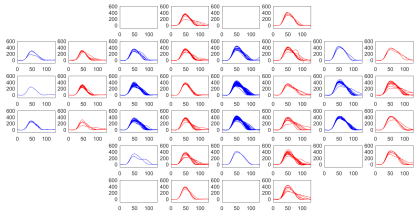

(a) Participant 9

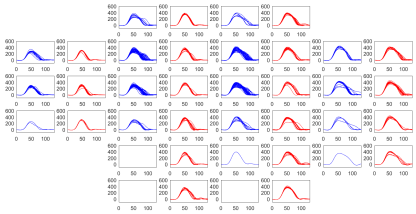

(b) Participant 10

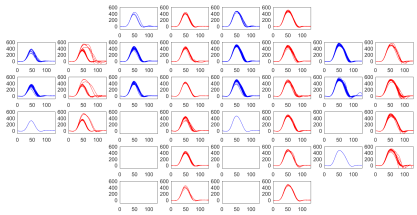

(c) Participant 11

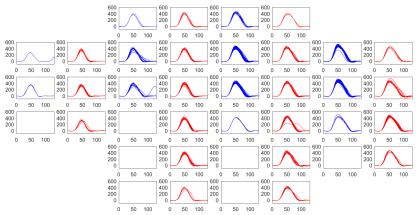

(d) Participant 12

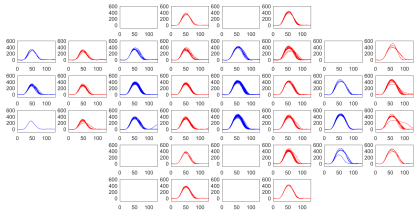

(e) Participant 13

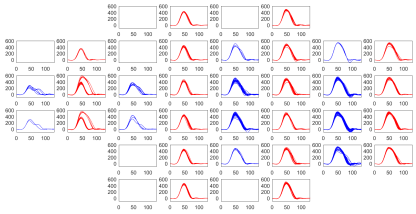

(f) Participant 14

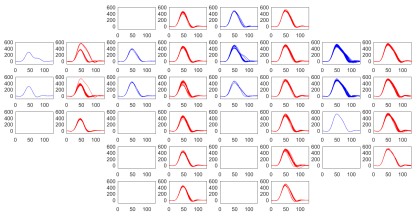

(g) Participant 15

Figure 5.3: Velocity profiles in the grid for all participants: Gabor in blue and control in red.

Bibliography

[1] A. Vince, *Fovea of the eye*, Apr. 2022. [Online]. Available: https://www.visioncenter.org/eye-anatomy/fovea.

[2] T. Biggs and S. McPhail, *Causes of color*, 1999. [Online]. Available: http://www.webexhibits.org/causesofcolor/1G.html.

[3] R. H. Wurtz, "Neuronal mechanisms of visual stability," *Vision Research*, vol. 48, pp. 2070–2089, Sep. 2008, ISSN: 00426989. DOI: 10.1016/j.visres.2008.03.021.

[4] B. Erdmann and R. Dodge, *Psychologische Untersuchungen über das Lesen auf experimenteller Grundlage*. Niemeyer, 1898.

[5] E. Matin, "Saccadic suppression: A review and an analysis," *Psychological Bulletin*, vol. 81, pp. 899–917, 12 1974.

[6] J. Ross, D. Burr, and C. Morrone, "Suppression of the magnocellular pathway during saccades," *Behavioural Brain Research*, vol. 80, pp. 1–8, 1996.

[7] R. John, M. M. Concetta, G. M. E, and B. D. C, "Response:'saccadicsuppression' – no need for an active extra-retinalmechanism," *TRENDS in Neurosciences*, vol. 24, pp. 317–318, 6 2001.

[8] M. R. Diamond, J. Ross, and M. C. Morrone, "Extraretinal control of saccadic suppression," *The Journal of Neuroscience*, vol. 20, pp. 3449–3455, 9 2000.

[9] J. Duqué, *Liepr1024 : Fondements neurophysiologiques et neuropsychologiques du système moteur - vision*, 2019.

[10] T. Yamasaki and S. Tobimatsu, *Motion perception in healthy humans and cognitive disorders*, 2011. DOI: 10.4018/978-1-60960-559-9.ch020.

[11] V. Dragoi, *Chapter 8: Ocular motor control*, Oct. 2020. [Online]. Available: https://nba.uth.tmc.edu/neuroscience/m/s3/chapter08.html.

[12] O. C and Students, *INTRODUCTION TO SENSATION AND PERCEPTION STUDENTS OF PSY 3031 AND EDITED BY DR. CHERYL OLMAN*. University of Minesota Libraries Publishing, 2022, pp. 338–340.

[13] R. Kleiser, R. J. Seitz, and B. Krekelberg, "Neural correlates of saccadic suppression in humans," *Current Biology*, vol. 14, pp. 386–390, Mar. 2004, ISSN: 09609822. DOI: 10.1016/j.cub.2004.02.036.

[14] C. Eric, J. Sebastien, and M. G. S, "'saccadic suppression' – no need for an active extra-retinal mechanism," *TRENDS in Neurosciences*, vol. 24, pp. 316–317, 6 2001.

[15] R. John, M. M. Concetta, G. E. Michael, and B. D. C., "Changes in visual perception at thetime of saccades," *TRENDS in Neurosciences*, vol. 24, pp. 113–121, 2 2001.

[16] K. V. Thilo, L. Santoro, V. Walsh, and C. Blakemore, "The site of saccadic suppression," *Nature Neuroscience*, vol. 7, pp. 13–14, 1 Jan. 2004, ISSN: 10976256. DOI: 10.1038/nn1171.

[17] A Thiele, P Henning, M Kubischik, and K.-P Hoffmann, "Neural mechanisms of saccadic suppression," 2002, pp. 2460–2462.

[18] F. Crevecoeur and K. P. Kording, *Saccadic suppression as a perceptual consequence of efficient sensorimotor estimation*, 2017. DOI: 10.7554/eLife.25073.001.

[19] B. Roberfroid, "Experimental testing of a sensorimotor origin of saccadic suppression," UCLouvain, 2018. [Online]. Available: https://dial.uclouvain.be/memoire/ucl/object/thesis:14750.

[20] S. R. Ltd, *Eyelink 1000 plus*, 2022.

[21] R. A. Becerra-García, R. García-Bermúdez, and G. Joya, "Differentiation of saccadic eye movement signals," *Sensors*, vol. 21, pp. 1–12, 5021 Aug. 2021, ISSN: 14248220. DOI: 10.3390/s21155021.

[22] Z Kapoula, "Evidence for a range effect in the saccadic system," *Vision Res*, vol. 25, pp. 1155–1157, 8 1985.

[23] Wikipedia contributors, *Student's t-test — Wikipedia, the free encyclopedia*, [Online; accessed 1-August-2022], 2022. [Online]. Available: https://en.wikipedia.org/w/index.php?title=Student%27s_t-test&oldid=1091184682.

[24] U. S. C. Group., *Introduction to linear mixed models*, 2021. [Online]. Available: https://stats.oarc.ucla.edu/other/mult-pkg/introduction-to-linear-mixed-models/.

[25] H. Collewijn, C. J. Erkelens, and R. M. Steinmant, "Binocular co-ordination of human horizontal saccadic eye movements," *Journal of Physiology*, vol. 404, pp. 157–182, 1988.

[26] H. Chen-Harris, W. M. Joiner, V. Ethier, D. S. Zee, and R. Shadmehr, "Adaptive control of saccades via internal feedback," *Journal of Neuroscience*, vol. 28, pp. 2804–2813, 11 Mar. 2008, ISSN: 02706474. DOI: 10.1523/JNEUROSCI.5300-07.2008.

[27] A. Goettker and K. R. Gegenfurtner, "A change in perspective: The interaction of saccadic and pursuit eye movements in oculomotor control and perception," *Vision Research*, vol. 188, pp. 283–296, Nov. 2021, ISSN: 18785646. DOI: 10.1016/j.visres.2021.08.004.

[28] J. J. O. D. Xivry and P. Lefèvre, *Saccades and pursuit: Two outcomes of a single sensorimotor process*, Oct. 2007. DOI: 10.1113/jphysiol.2007.139881.

[29] R. J. Krauzlis, *Recasting the smooth pursuit eye movement system*, Feb. 2004. DOI: 10.1152/jn.00801.2003.

[30] N. J. Priebe and S. G. Lisberger, "Estimating target speed from the population response in visual area mt," *Journal of Neuroscience*, vol. 24, pp. 1907–1916, 8 Feb. 2004, ISSN: 02706474. DOI: 10.1523/JNEUROSCI.4233-03.2004.

UNIVERSITÉ CATHOLIQUE DE LOUVAIN
École polytechnique de Louvain
Rue Archimède, 1 bte L6.11.01, 1348 Louvain-la-Neuve, Belgique | **www.uclouvain.be/epl**